# Simplified models of flue instruments: Influence of mouth geometry on the sound source

S. Dequand, J. F. H. Willems, M. Leroux, R. Vullings, M. van Weert, C. Thieulot, and A. Hirschberg[a)]
*Technische Universiteit Eindhoven, Postbus 513, 5600 MB Eindhoven, The Netherlands*

(Received 12 December 2001; revised 27 November 2002; accepted 16 December 2002)

Flue instruments such as the recorder flute and the transverse flute have different mouth geometries and acoustical response. The effect of the mouth geometry is studied by considering the aeroacoustical response of a simple whistle. The labium of a transverse flute has a large edge angle (60°) compared to that of a recorder flute (15°). Furthermore, the ratio $W/h$ of the mouth width $W$ to the jet thickness $h$ can be varied in the transverse flute (lips of the musician) while it is fixed to a value $W/h \approx 4$ in a recorder flute. A systematic experimental study of the steady oscillation behavior has been carried out. Results of acoustical pressure measurements and flow visualization are presented. The sharp edge of the recorder provides a sound source which is rich in harmonics at the cost of stability. The larger angle of the labium of the flute seems to be motivated by a better stability of the oscillations for thick jets but could also be motivated by a reduction of broadband turbulence noise. We propose two simplified sound source models which could be used for sound synthesis: a jet-drive model for $W/h > 2$ and a discrete-vortex model for $W/h < 2$. © *2003 Acoustical Society of America.* [DOI: 10.1121/1.1543929]

PACS numbers: 43.75.Np, 43.75.Qr [NHF]

## I. INTRODUCTION

In a flue instrument, the sound is produced by the interaction of a jet with a sharp edge (called the labium) placed in the opening (mouth) of a resonator (body of the instrument). The jet is formed by flow separation at the end of a slit (the flue channel) and travels along the mouth of the resonator towards the labium. Coupling between jet oscillations in the mouth and acoustical resonances in the body provides self-sustained oscillations of the jet and maintains sound production.

A large variety of flue instruments are discussed by, among others, Castellengo (1976), Campbell and Greated (1987), and Fletcher and Rossing (1998). In a recent review, Fabre and Hirschberg (2000) discuss the literature on physical modeling of flue instruments. As explained in their paper, there exist no accurate models for the flow in the mouth of such instruments. Formal theories of Crighton (1992), Elder (1992), and Howe (1998) are based on a linear response of very crude models of the flow. They cannot predict the amplitude of the oscillations. We therefore use here modifications of simplified nonlinear models. Next to their passive acoustical behavior, which can be described by means of simple acoustical models (Fletcher and Rossing, 1998; Coltman, 1966; Nederveen, 1998; Wolfe, 2001), flue instruments distinguish themselves also by significantly different mouth geometries. Simple models for the source are found in literature. Coltman (1968, 1969, 1976) developed a simplified model of the sound production which is called the jet-drive model. A similar model was used by Powell (1961) to predict the sound production of an edge-tone system. In this model, the jet flow $Q_j$ is separated at the labium into a flow $Q_{\text{in}}$ entering the resonator and a flow $Q_{\text{out}}$ leaving the resonator. These flows act as two complementary monopole sound sources ($Q_j = Q_{\text{in}} + Q_{\text{out}}$) (Elder, 1973). This jet-drive model is commonly accepted in the literature (Fletcher and Rossing, 1998). In its original form, the jet-drive model includes a momentum drive associated to the volume injection. Coltman (1980) has shown that this effect is much weaker than predicted by the quasi-steady model of Fletcher and Rossing (1998) and Elder (1973). We will therefore ignore this momentum drive. Fabre *et al.* (1996) and Verge *et al.* (1997a, b), however, demonstrated that vortex shedding at the labium was a key damping mechanism and proposed simplified models for this. When this modified jet-drive model (without momentum drive but with vortex damping) is implemented in a global model of the instrument, one can predict within 1 dB the oscillation amplitudes in a recorderlike instrument (Verge *et al.*, 1997a, b; Fabre *et al.*, 1996) at low Strouhal numbers corresponding to the first hydrodynamic mode of the jet. For higher values of the Strouhal number, the jet-drive concept appears to fail as a result of the breakdown of the jet into discrete vortices. This effect was first reported by Fletcher (1976). In the case of a jet/labium configuration without resonator (edge-tone), Holger *et al.* (1977) proposed to describe the jet flow behavior in terms of a Von Kàrmàn vortex street. The model of Holger (1977) has recently be used with some success by Ségoufin *et al.* (2001). While the idea of using such a discrete-vortex model for a flue instrument at high Strouhal numbers was proposed earlier (Hirschberg, 1995; Fabre and Hirschberg 2000), it was only recently used for a whistle by Meissner (2002) in the case of a very thin jet compared to the mouth width. In the present paper, we investigate the use of the combination of a similar discrete-vortex model and the jet-drive model in order to explain the effect of the ratio between the mouth width $W$ and the jet height $h$ on the flow behavior in a simple whistle.

[a)]Author to whom correspondence should be addressed. Electronic mail: a.hirschberg@tue.nl

 0001-4966/2003/113(3)/1724/12/$19.00 

In order to simplify the theory, we consider only the maximum of the dimensionless amplitude which corresponds to a critical Strouhal number at which the sound source is in phase with the acoustical velocity through the mouth. We therefore avoid in the jet-drive model the description of the phase lag due to the jet response.

Furthermore, we describe some experimental results obtained from a study of the effect of the mouth geometry on the oscillation amplitude and its stability. The pulsation amplitudes predicted by our model as a function of the ratio $W/h$ between the mouth width $W$ and the jet thickness $h$ are compared to experimental results. The model is described in Sec. II and the experimental work is presented in Sec. III. This includes some flow visualization.

## II. SIMPLE MODELS

In this section, we propose a simple model to predict the pulsation amplitudes in a whistle (or ocarina). This flue instrument can be represented, in a first approximation, by a resonator with a closed volume $V=H^2\times L$ (where $H^2$ and $L$ are the square cross-section and the length of the cavity, respectively) and a mouth opening of cross-section $S_m=H\times W$ along which a jet is grazing (where $W$ is the width of the mouth opening). The system has a single acoustic mode behavior. The excitation of the resonator by the jet oscillations is represented by either a jet-drive model or a discrete-vortex model (Sec. II C).

### A. Single mode model

As explained in a previous study on self-sustained oscillations in a Helmholtz-like resonator (Dequand, 2001, 2001b), the resonator is described as a mass-spring system where the mass represents the incompressible flow in the neck of the resonator (small pipe of length $L_m$ and cross-section area $S_m$), and the spring represents the volume $V$ of the resonator. This volume is not shallow and plane waves can propagate inside. Such a system could be called a ''stopped pipe.'' By considering the particle displacement $\zeta$ in the neck (mouth) of the resonator (defined positive when it is directed into the volume $V$), Newton's law yields

$$M_a\frac{d^2\xi}{dt^2}+R\frac{d\xi}{dt}+K\xi=\mathcal{F}(t), \tag{1}$$

where $\mathcal{F}(t)$ denotes the aeroacoustical forces acting on the resonator and will be determined in the next paragraph. The mass $M_a$ is related to the effective length $L_{\text{eff}}$ of the neck (mouth) of the resonator:

$$M_a=\rho_0 L_{\text{eff}}HW, \tag{2}$$

where $\rho_0$ is the uniform flow density.

By applying the momentum conservation to the neck, the effective length of the neck is expressed as

$$L_{\text{eff}}=\frac{1}{2\pi f_1\rho_0}\left|\frac{p'}{u'}\right|, \tag{3}$$

where $u'$ and $p'$ are the acoustical perturbations of the velocity and the pressure, respectively. Then, by writing the mass conservation between the resonator and the neck and assuming that only plane waves $p^+$ and $p^-$ propagate in the resonator [$W\rho_0 c_0 u'=H(p^+-p^-)$ where $c_0$ is the speed of sound], the effective length $L_{\text{eff}}$ becomes

$$L_{\text{eff}}=\frac{W}{H}\frac{c_0}{2\pi f_1}\left|\frac{p^++p^-}{p^+-p^-}\right|=\frac{W}{H}\frac{c_0}{2\pi f_1}\cot\left(\frac{2\pi f_1}{c_0}L\right). \tag{4}$$

The damping coefficient $R$ is related to the quality factor $Q_f=f_1/\Delta f_1$:

$$R=\frac{2\pi f_1 M_a}{Q_f}. \tag{5}$$

The quality factor $Q_f=30$ was determined experimentally from measurement of the 3-dB width $\Delta f_1$ of the resonance peak at $f_1$. By definition, the spring constant $K$ is

$$K=M_a(2\pi f_1)^2. \tag{6}$$

In Eqs. (2)–(6), the frequency $f_1$ is measured. In the next sections, we will omit the subscript 1 and we will denote the frequency by $f$. In the present work, we identified $f_1$ with the whistling frequency at the maximum amplitude of a mode.

### B. Losses induced by vortex shedding at the labium

Flow separation occurs at the sharp edge of the labium. We consider here the vortex shedding associated with the quasi-steady flow separation of the acoustical flow through the mouth (Fabre, 1996; Verge *et al.*, 1997a, b).

By assuming that the flow separation of the acoustic flow $Q=(d\xi/dt)HW$ (where $HW$ is the cross-sectional area of the mouth) at the labium results in the formation of a free jet [quasi-steady free-jet model proposed by Ingard and Ising (1967)], the effects of vortices can be represented by a fluctuating pressure $\Delta p_v$ across the mouth of the instrument:

$$\Delta p_v=-\frac{1}{2}\rho_0\left(\frac{Q}{\alpha_v HW}\right)^2\text{sign}(Q), \tag{7}$$

where $\alpha_v$ is the vena-contracta factor of the jet. We choose the value of $\alpha_v=0.6$ as used by Verge *et al.* (1997a, b). The time-averaged power losses induced by the vortex shedding at the labium is then

$$\langle\mathcal{P}_{\text{losses}}\rangle=\langle\Delta p_v Q\rangle=-\frac{1}{2T}\frac{\rho_0 HW}{\alpha_v^2}\int_0^T\left(\frac{d\xi}{dt}\right)^2\left|\frac{d\xi}{dt}\right|dt. \tag{8}$$

Howe (1975) proposed to use the point vortex model of Brown and Michael (1954) in order to describe the vortex shedding at the labium. Using an asymptotic approximation, he obtains an analytical model which predicts a sound production by this vortex shedding. A great advantage of the model proposed by Howe (1975) is that it could explain the difference in generation of harmonics on the sharpness of the edge of the labium as proposed by Nolle (1983). The classical model of Fletcher and Rossing (1998) does not predict an effect of the edge geometry. The model of Howe (1975) can easily be generalized to be applied to an arbitrary edge angle as long as the vortex remains close to the labium. While self-similar solutions of Pullin (1978) and Peters (1993) are available, we expect that a numerical simulation of the vortex path as a function of time is useful. The numerical study of Dequand (2001, 2001b) indicates significant discrepancies

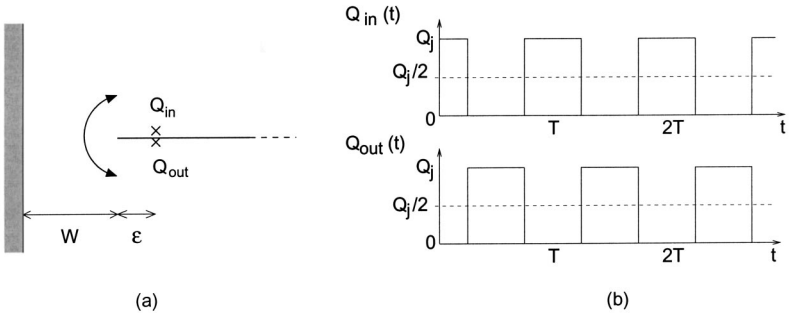


FIG. 1. (a) Idealized representation of the mouth of the instrument in the jet-drive model (Verge *et al.*, 1994a) and (b) time dependence of the two complementary sources $Q_{\text{in}}$ and $Q_{\text{out}}$.

between the asymptotic analytical solution of Howe (1975) and a numerical solution. From simple scaling arguments one can, however, expect without calculations that a sharper edge as found in the recorder will produce a more abrupt and stronger absorption than an edge of 60° as found in the flute. The choice of the sharp labium in the recorder might therefore be dictated by the necessity of a stronger production of higher harmonics.

### C. Simple source models

#### *1. Jet-drive model*

The mouth of the resonator can be described as a two-dimensional slit of width $W$ between a wall and a semi-infinite plane (perpendicular to the wall) representing the labium (Fig. 1). The jet volume flow is assumed to be split into two complementary monopole (line) sources $Q_{\text{in}}=|Q_j|e^{i\omega t}=-Q_{\text{out}}$ placed at a distance $\epsilon$ from the edge of the labium at the lower and upper side of the labium, respectively. This jet-drive model has been used by Verge *et al.* (1994a) for small jet thickness $h_j$ compared to the mouth width $W$. The source is represented by a fluctuating pressure $\Delta p_j$ deduced from the potential difference across the mouth induced by two monopoles:

$$\Delta p_j \approx \rho_0 \frac{\delta_j}{HW}\frac{dQ_j}{dt}, \tag{9}$$

where $\delta_j$ is the effective distance between the two complementary monopole sources $Q_{\text{in}}$ and $Q_{\text{out}}$. The length $\delta_j$ is calculated by means of a potential flow theory. For the limit $\epsilon \ll W$, we have, following Verge *et al.* (1994a, b),

$$\frac{\delta_j}{W} \approx \frac{4}{\pi}\sqrt{\frac{2\epsilon}{W}}. \tag{10}$$

In the thin jet limit ($W/h \gg 1$), the only length scale in the flow around the edge of the labium is the jet thickness $h_j$, so that $\epsilon$ should be proportional to $h_j$. Verge *et al.* (1994a, b) actually assume that $\epsilon = h_j$. We make an additional approximation by identifying the jet thickness $h_j$ with the height $h$ of the flue channel. Hence, we neglect the lateral broadening of the jet velocity profile as the jet travels across the mouth.

The power generated by the source is calculated by assuming that the acoustical flow is locally a two-dimensional incompressible flow and that the source is in phase with the acoustical flux through the mouth $Q=(d\xi/dt)WH$ (where $WH$ is the cross-sectional area of the mouth). This corresponds to the condition for which the oscillation amplitude has a maximum as a function of the blowing pressure. This assumption allows us to ignore the effect of the jet response on the phase lag between the sound source and the acoustical flow velocity oscillation. We assume also that for each half oscillation period, the jet direction alternates between inside and outside the resonator. The passage of the jet from one side to the other side of the labium is assumed to be within a very short time compared to the oscillation period. The sources $Q_{\text{in}}$ and $Q_{\text{out}}$ behave in terms of the time as a square wave of amplitude $Q_j/2$ [Fig. 1(b)]:

$$Q_{\text{in}} = \frac{Q_j}{2} + Q'_{\text{in}}, \quad Q_{\text{out}} = \frac{Q_j}{2} + Q'_{\text{out}}. \tag{11}$$

This model should be reasonable for large displacements of the jet at the labium which are observed in our visualizations for $W/h > 2$.

As explained above, the sources $Q_{\text{in}}$ and $Q_{\text{out}}$ have an opposite phase ($Q'_{\text{out}} = -Q'_{\text{in}}$) because $Q_j$ is constant ($Q_j = Q_{\text{in}} + Q_{\text{out}}$). The average over an oscillation period $T$ of the power generated by this jet drive is then

$$\begin{aligned}\langle \mathcal{P}_{\text{jet-drive}} \rangle &= \langle \Delta p_j Q \rangle \\ &= \frac{2}{TH}\int_0^{T/2} \rho_0 \frac{4}{\pi}\sqrt{\frac{2h}{W}}|Q_j|\,\delta\left(t-\frac{T}{4}\right)\left(\frac{d\xi}{dt}\right)HW\,dt \\ &= \frac{8}{\pi T}\rho_0\sqrt{\frac{2h}{W}}U_0 hHW\left|\frac{d\xi}{dt}\right|,\end{aligned} \tag{12}$$

where $U_0$ is the jet flow velocity.

By balancing the acoustical energy losses $\langle \mathcal{P}_{\text{losses}} \rangle$ due to vortex-shedding at the labium [Eq. (8)] to the acoustic energy produced by the jet $\langle \mathcal{P}_{\text{jet-drive}} \rangle$ [Eq. (12)], Verge *et al.* (1997a, b) found a relation between the pulsation amplitude $(d\xi/dt)_{\max}$, the Strouhal number $S_r = fW/U_0$, and the ratio $W/h$ of the mouth width $W$ and the jet thickness $h$:

$$\left(\frac{(d\xi/dt)_{\max}}{U_0}\right)^2 \sim S_r\left(\frac{h}{W}\right)^{3/2}. \tag{13}$$

The agreement of our experimental data with this relationship will be checked in Sec. III (Fig. 11).

While we have assumed that $W/h \gg 1$, we also have assumed that the jet does not break down into discrete vortices. This is only reasonable for the first hydrodynamic mode $S_r = fW/U_0 < 0.3$. As observed by Fletcher (1976), a jet-drive model as proposed here would severely overestimate sound production by higher-order hydrodynamic modes of the jet

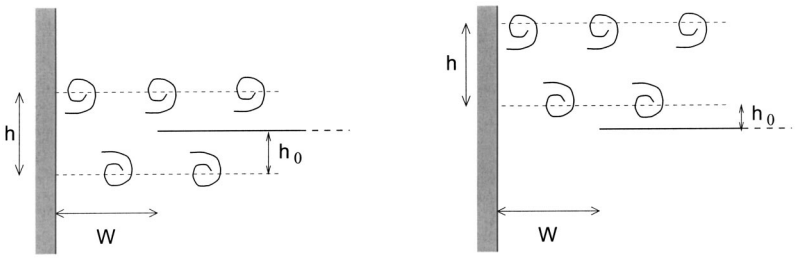


FIG. 2. Idealized representation of the mouth of the instrument in the discrete-vortex model. The two shear layers are separated by a distance $h$ and the parameter $h_0$ represents the distance between the outer shear layer and the labium.

oscillation. For higher-order modes, a discrete-vortex model should be used. The use of Holger's model (Holger *et al.*, 1977) could be considered here.

### 2. Discrete-vortex model

When the jet is thick, it will appear from experimental observations that the grazing jet flow is not fully deflected into the resonator. A description in terms of the jet-drive model becomes difficult. If the jet is very thick, the two shear layers bounding the jet behave independently of each other. We follow here the idea of Meissner (2002) to describe both shear layers bounding the jet in terms of discrete vortices. This corresponds to the application of Nelson's model (Nelson *et al.*, 1983; Hirschberg, 1995; Dequand, 2001) to each shear layer. As in the jet-drive model described in the previous section, the mouth of the resonator is described as a two-dimensional slit of width $W$ between a wall and a semi-infinite plane representing the labium (Fig. 2). In Nelson's model (Nelson *et al.*, 1983), the vorticity of the shear layers of the jet is assumed to be concentrated into line vortices traveling along straight lines (in the axis direction of the flue channel) with a constant velocity $U_\Gamma = 0.4U_0$. This value of $U_\Gamma$ corresponds to experimental observations (Bruggeman *et al.*, 1989). We assume that the circulation of the vortices grows linearly during the first period of their life (before remaining constant).

The two shear layers are separated from each other by a distance $h$ which is assumed to be constant and equal to the jet thickness at the flue exit. In order to avoid the singularity at the labium, the positions of the two shear layers are chosen such that the vortices pass along the labium but do not hit the labium (Fig. 2). We introduce the parameter $h_0$ corresponding to the distance between the lower shear layer and the labium. The value of $h_0$ is not critical when varied in the range $W/10 \leqslant h_0 \leqslant W/4$. In the results presented, we used $h_0 = W/5$.

The generation of vortices is periodic and is triggered by the acoustical flux through the mouth. A new vortex is formed at the inner shear layer (on the resonator side) each time the acoustical velocity $d\xi/dt$ changes sign from directed towards the outside to directed towards the inside of the resonator [minimum of the acoustical pressure $p'(L)$ in the resonator]. A new vortex is formed at the outer shear layer half an oscillation period later [maximum of the acoustical pressure $p'(L)$ in the resonator]. The circulation of the $j$th vortex (with $j=1,2,3,...$) at the inner shear layer ($\Gamma_i^{(j)}$) and at the outer shear layer ($\Gamma_o^{(j)}$) can be written as

$$
\begin{aligned}
&\Gamma_i^{(j)}(t) = \frac{U_0^2}{2}[t-(j-1)T] \quad \text{for } (j-1)T \leqslant t \leqslant jT,\\
&\Gamma_i^{(j)}(t) = \frac{U_0^2}{2}T \quad \text{for } t > jT,\\
&\Gamma_o^{(j)}(t) = -\frac{U_0^2}{2}[t-(2j-1)T/2]\\
&\qquad\qquad \text{for } (2j-1)T/2 \leqslant t \leqslant (2j+1)T/2,\\
&\Gamma_o^{(j)}(t) = -\frac{U_0^2}{2}T \quad \text{for } t > (2j+1)T/2,
\end{aligned}
\tag{14}
$$

where $T$ is the oscillation period.

The acoustical power generated by the vortices is calculated by using Howe's energy corollary (Howe, 1980). The acoustical power averaged over one period of oscillations $T$ is

$$
\langle \mathcal{P}_{\text{discrete-vortex}} \rangle = \frac{-\rho_0}{T}\int_0^T \int_{V_S} (\boldsymbol{\omega}\times\mathbf{v})\cdot\mathbf{u}'\, dV\, dt, \tag{15}
$$

where the volume integration is taken over the source region of volume $V_S$ and where the local acoustical flow velocity $\mathbf{u}'$ represents the unsteady part of the potential flow component of the velocity field $\mathbf{v}$.

The vorticity field $\boldsymbol{\omega} = \boldsymbol{\nabla}\times\mathbf{v}$ takes into account the contribution of each vortex of the shear layers:

$$
\boldsymbol{\omega} = \sum_j [\Gamma_i^{(j)}(t)\,\delta(\mathbf{x}-\mathbf{x}_i^{(j)}(t)) + \Gamma_o^{(j)}(t)\,\delta(\mathbf{x}-\mathbf{x}_o^{(j)}(t))]. \tag{16}
$$

The complex conjugate of the local acoustical flow velocity $\mathbf{u}'$ can be determined by means of potential flow theory (Verge *et al.*, 1994a, b; Dequand, 2001, 2001b):

$$
u'^* = \frac{4}{\pi}\frac{d\xi}{dt}\frac{\zeta}{\zeta^2-1}, \tag{17}
$$

where $\zeta = z/W \pm \sqrt{(z/W)^2-1}$ is either the transformation of the upper half of the $\zeta$-plane into the upper half of the real $z$-plane (positive sign) or the transformation into points of the lower half of the real $z$-plane (negative sign) (Fig. 3).

This method takes into account the nonuniformity of the acoustical velocity $\mathbf{u}'$, which is not considered by Meissner (2002) or Hirschberg (1995).

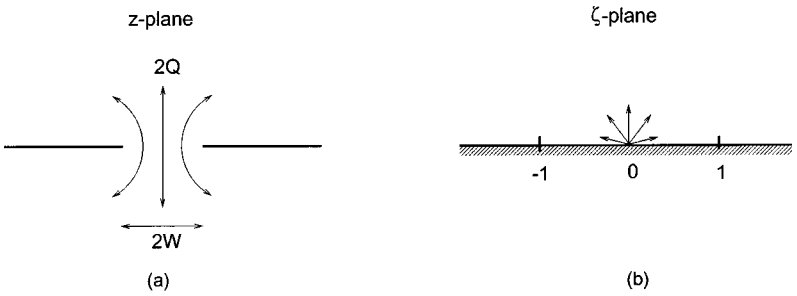


FIG. 3. (a) Idealized geometry deduced from the actual geometry by means of the method of images ($z$-plane) and (b) transformed plane by means of a conformal mapping ($\zeta$-plane).

#### *3. Global source model*

The jet-drive model, valid for thin jets, and the discrete-vortex model, valid for thick jets, can be combined in a global model in which the acoustical power generated by the source is defined as

$$\langle \mathcal{P}_{\text{source}} \rangle = \frac{(W/h)^3 \langle \mathcal{P}_{\text{jet-drive}} \rangle + (W/h)_0^3 \langle \mathcal{P}_{\text{discrete-vortex}} \rangle}{(W/h)^3 + (W/h)_0^3}, \tag{18}$$

where $(W/h)_0$ is a fit parameter. We could choose $(W/h)_0 = 2.5$, which is the value of $W/h$ for which both models (jet-drive and discrete-vortex) give the same source power.

### D. Energy balance

Assuming that the particle displacement $\xi$ in the neck is harmonic $\xi(t) = -\hat{\xi}\cos \omega t$, we can write the energy balance of the system from Eqs. (1), (8), and (18). The amplitude $|d\xi/dt|/U_0$ of the oscillations can then be deduced as a function of the Strouhal number $S_r = fW/U_0$.

## III. EXPERIMENTAL STUDY

### A. Experimental setup

A scheme of the experimental setup is shown in Fig. 4. The resonator is placed in a semi-anechoic room, 60 mm downstream of the outlet (square cross-sectional area of 60 $\times 60\ \text{mm}^2$) of a silent wind tunnel. The resonator volume consists out of an aluminum pipe of square cross-sectional area of $H^2 = 60 \times 60\ \text{mm}^2$ and 2 mm wall thickness. Metal plates of 3 mm wall thickness are glued on the pipe walls to reduce potential wall vibrations. The pipe is terminated by a piston in which a piezo-electrical transducer (PCB 116A with Kistler Charge amplifier type 5007) is placed. The piston position can be varied and is determined within 1 mm.

The main pipe, which carries the grazing flow, is terminated 4.9 cm upstream of the neck of the resonator. In the region where the vortices are formed, the side walls of the resonator are made of glass windows.

The mouth consists of three blocks which can be changed to modify the mouth geometry. The instrument is driven by a free jet of thickness $h$ formed by blowing through a slit (flue channel) of height $h$. This height $h$ was varied between 2 and 60 mm. The slit or flue channel was made by the aperture between a block (lip) of 2.5 cm width and the upstream block of the neck of the cavity. The upstream side of the lip was rounded in order to avoid flow separation within the flue channel, while the downstream side was either sharp [Fig. 5(a)] or chamfered at an angle of 45° [Fig. 5(b)]. Two different angles ($\alpha = -15°$ and 60°) of labium were used. Note that the 15°-labium is directed outside of the cavity while the 60°-labium is directed inside the cavity. These configurations (angle of the labium and direction) correspond to the mouth of a transverse flute and of a recorder, respectively. The distance $W$ between the flue channel exit and the labium was either 24 mm for the 60°-labium or 20 mm for the 15°-labium for a flue exit with sharp edges. With edges, the distance $W$ was increased by 6 mm to 30 and 26 mm, respectively, for the two different labia. In the region surrounding the mouth of the resonator, the side walls of the resonator are made up of glass windows to allow for flow visualization.

### B. Acoustical measurements

During the acoustical measurements, the amplitude of the acoustical pressure $p'_{\text{exp}}$ at the top of the resonator, the frequency of the acoustical oscillations $f$, the length $L$ of the resonator, and the jet flow velocity $U_0$ were determined. As we consider low frequencies, only plane waves propagate in the cavity of the resonator. The mean acoustical velocity amplitude $|d\xi/dt|$ (defined as the ratio between the acoustical flux through the mouth and the mouth opening area $H \times W$) can then be deduced by the formula

$$\frac{d\xi}{dt} = \frac{H}{W} \frac{|p'_{\text{exp}}|}{\rho_0 c_0} \sin\left(\frac{2\pi f L}{c_0}\right) \sin(2\pi f t). \tag{19}$$

#### *1. Experimental results*

The measured pulsation amplitudes $|d\xi/dt|/U_0$ as a function of the Strouhal number $S_r = fW/U_0$ are shown in Figs. 6–9 for the four different configurations: the 15°-

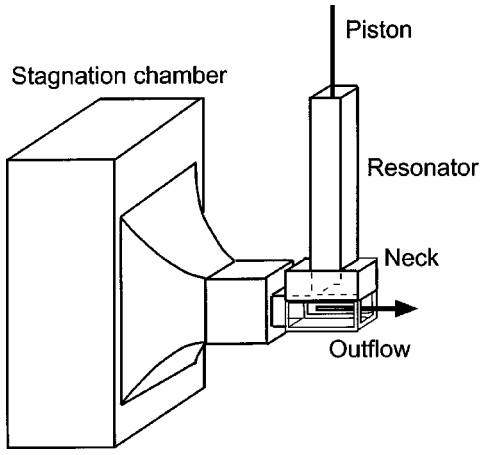


FIG. 4. Experimental setup.

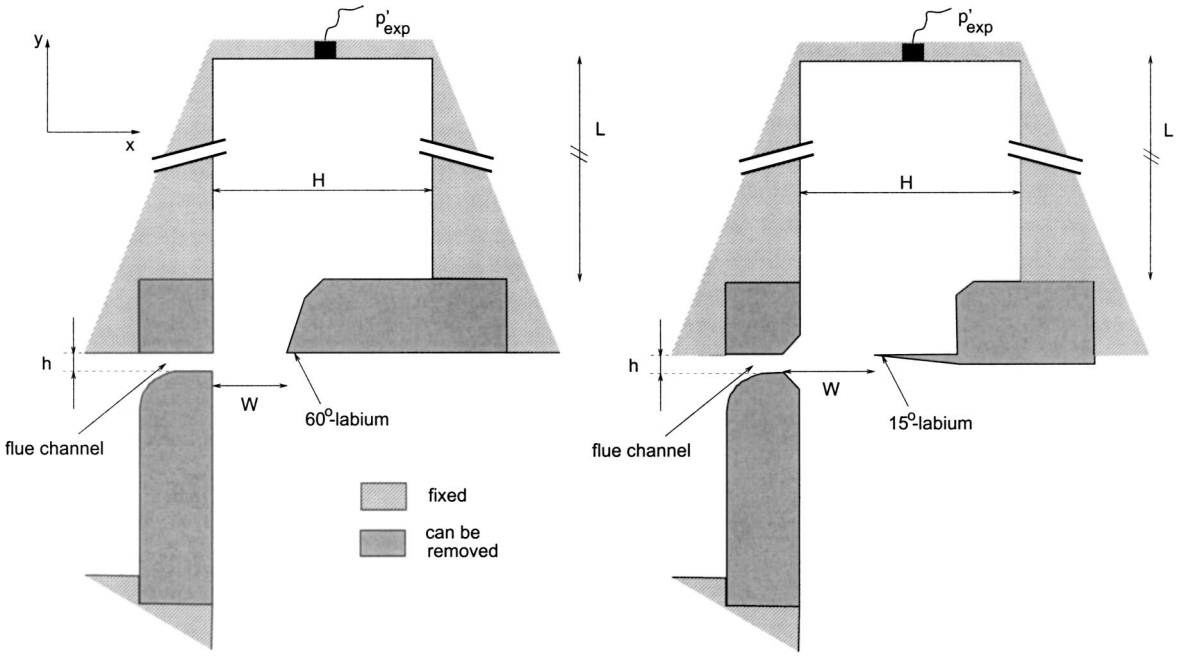


FIG. 5. Mouth geometry. (left) Flue exit with sharp edges and 60°-labium and (right) flue exit with chamfered edges and 15°-labium.

labium and the 60°-labium with either chamfered (Fig. 6 and 8) or sharp lips (Figs. 7 and 9). The results are presented for different heights $h$ of the flue channel. We observe that for thick jets ($h \geqslant 10$ mm), the measured pulsation amplitudes are much less sensitive to the choice of $h$ than for thinner jets.

From the experimental data shown in Figs. 6–9, the maximum of the pulsation amplitudes $(|d\xi/dt|/U_0)_{\max}$ can be deduced and plotted as a function of the ratio $W/h$ of the width $W$ of the mouth opening and the height $h$ of the flue channel. The results are presented in Fig. 10 for the four configurations.

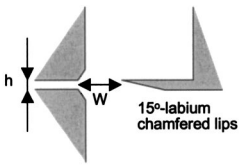


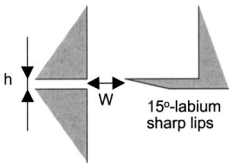


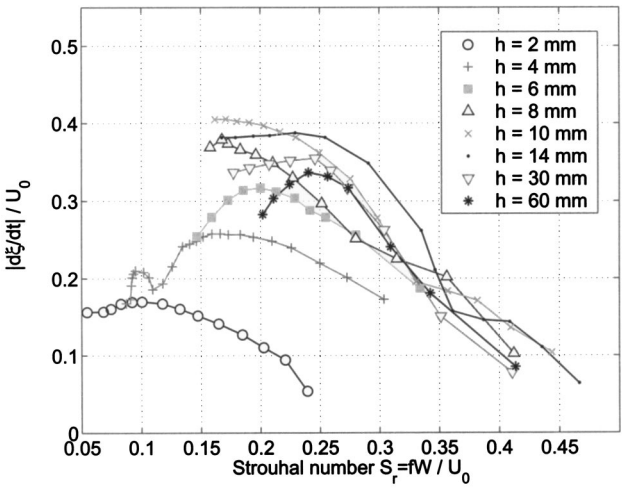


FIG. 6. The 15°-labium with chamfered lips. Pulsation amplitudes $|d\xi/dt|/U_0$ in terms of the Strouhal number $S_r = fW/U_0$ based on the mouth width $W = 26$ mm (length of the resonator $L = 191$ mm).

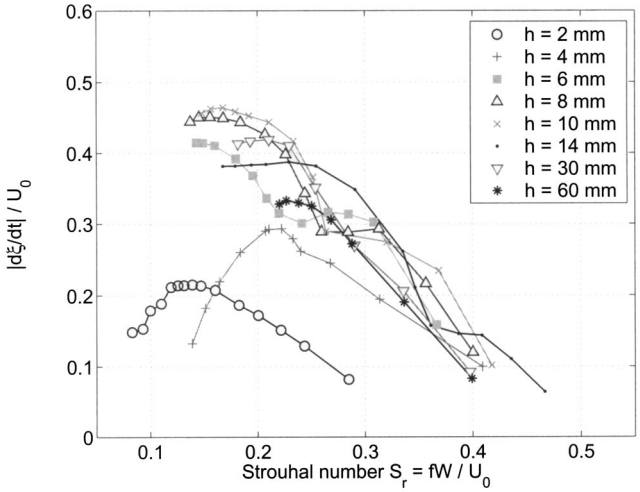


FIG. 7. The 15°-labium with sharp lips. Pulsation amplitudes $|d\xi/dt|/U_0$ in terms of the Strouhal number $S_r = fW/U_0$ based on the mouth width $W = 20$ mm (length of the resonator $L = 191$ mm).

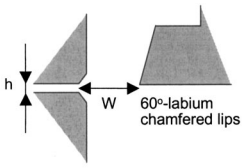


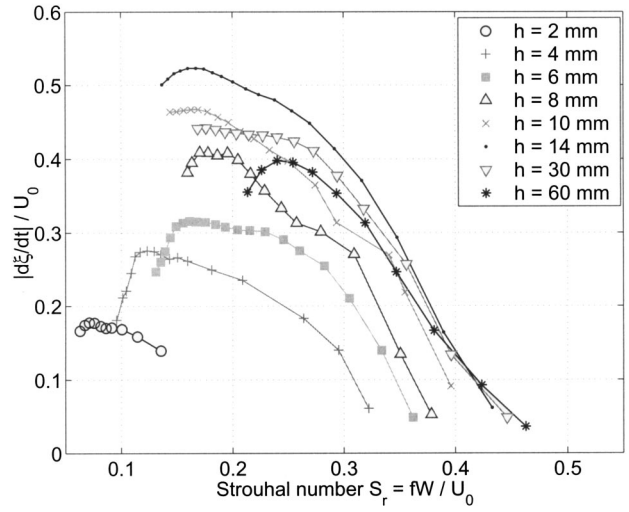


FIG. 8. The 60°-labium with chamfered lips. Pulsation amplitudes $|d\xi/dt|/U_0$ in terms of the Strouhal number $S_r = fW/U_0$ based on the mouth width $W = 30$ mm (length of the resonator $L = 191$ mm).

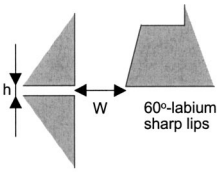


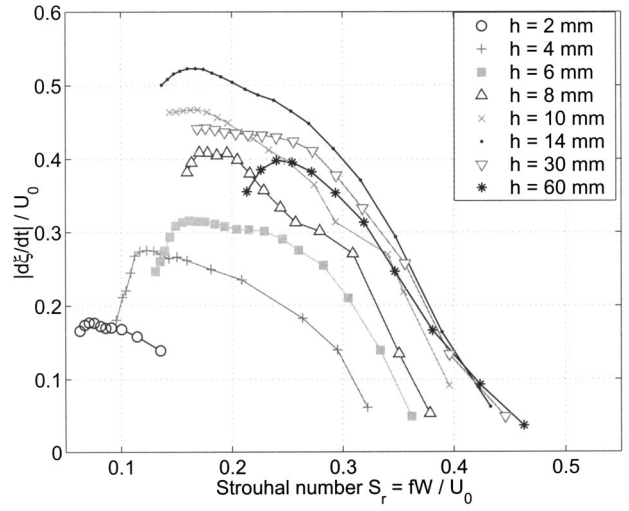


FIG. 9. The 60°-labium with sharp lips. Pulsation amplitudes $|d\xi/dt|/U_0$ in terms of the Strouhal number $S_r = fW/U_0$ based on the mouth width $W = 24$ mm (length of the resonator $L = 191$ mm).

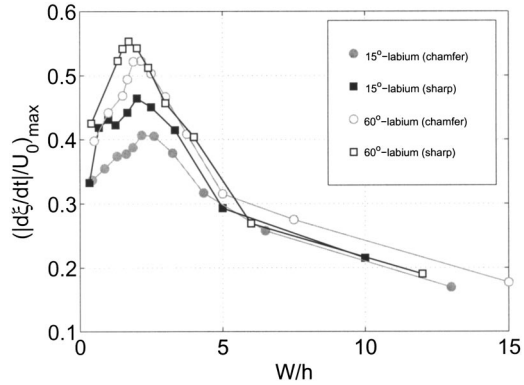


FIG. 10. Maximum of the dimensionless acoustical velocity amplitude $(|d\xi/dt|/U_0)_{\max}$ as a function of the ratio $W/h$ between the width $W$ of the mouth opening and the height $h$ of the flue channel. The data are shown for a flue exit with sharp and chamfered edges and for both the 15° and 60°-labia (length of the resonator $L = 191$ mm).

We observe that the maximum of amplitude $(|d\xi/dt|/U_0)_{\max}$ reached for the 60°-labium is 20% higher than that obtained for the 15°-labium. This difference in amplitude can be explained by the fact that in the case of the 15°-labium, the losses due to vortex shedding at the labium are more important than for the 60°-labium. This difference in amplitude is also observed for real musical instruments as the flute (60°-labium) and the recorder flute (15°-labium). A maximum of the amplitude $(|d\xi/dt|/U_0)_{\max}$ is reached for a ratio $W/h$ around 2. It is interesting to note (Fletcher, 2002) that this corresponds roughly to the maximum of instability for an infinite profile with a Bickley velocity profile (Mattingly and Criminale, 1971) at a hydrodynamical wave number $\pi/(2W)$. Furthermore, when the edges of the flue exit are sharp, the pulsation amplitudes are higher than for a chamfered flue exit. This effect of the geometry of the flue exit has also been observed by Ségoufin *et al.* (2000). In the case of the 15°-labium and a flue exit with sharp edges (Fig. 7), we observe also some instabilities in the measured pulsa-

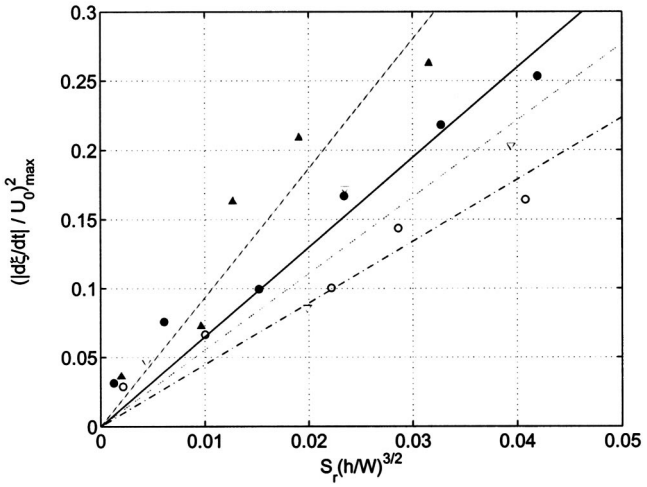


FIG. 11. Jet-drive model for thin jets $(W/h > 2)$. Experimental data (points) are compared with a fit (lines) of the relation found by Verge *et al.* 1997a, b [Eq. (13)] for the four different mouth geometries: 60°-labium and flue exit with chamfered edges (●, ———), 60°-labium and flue exit with sharp edges (▲, ———), 15°-labium and flue exit with chamfered edges (○, ·–·–) and 15°-labium and flue exit with sharp edges (▽, – – –).

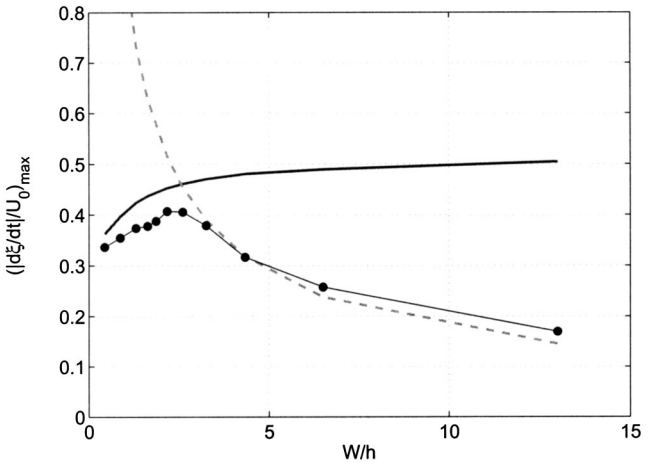


FIG. 12. Maximum of the dimensionless acoustical velocity amplitude $(|d\xi/dt|/U_0)_{\max}$ as a function of the ratio $W/h$ between the width $W$ of the mouth opening and the height $h$ of the flue channel. The data are shown for a flue exit with chamfered edges and for the 15°-labium. Experimental data (●) are compared to the values predicted by means of the proposed analytical models: discrete-vortex model (———) and jet-drive model (– – –). In the discrete-vortex model, the distance between the lower shear layer and the labium is set to $h_0=5$ mm (Fig. 2).

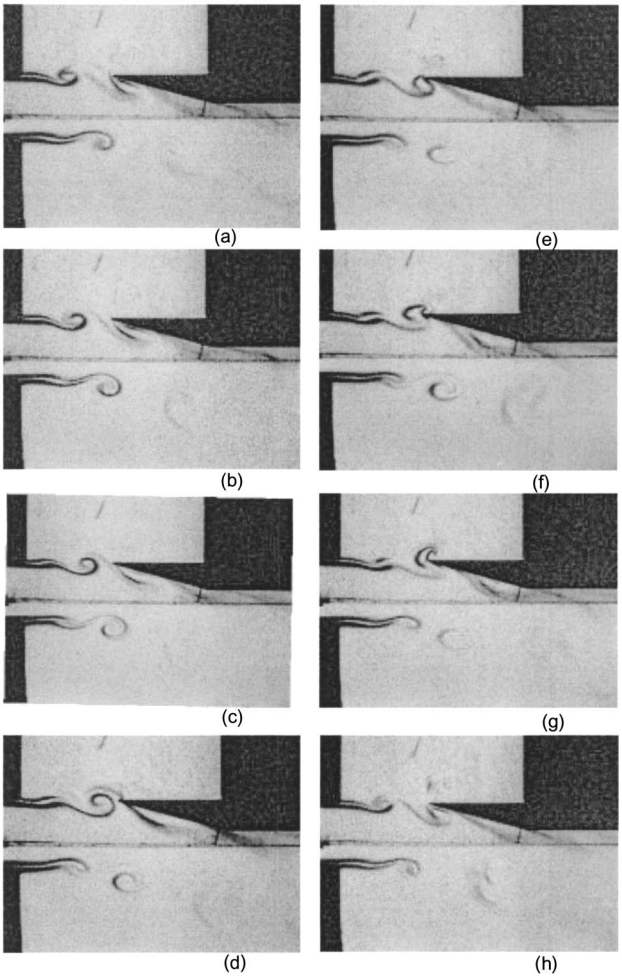


FIG. 13. Flow separation at the 15°-labium of the resonator induced by the passage of vortices near the labium. This behavior was also observed by Verge (1997a, b) for a recorder.

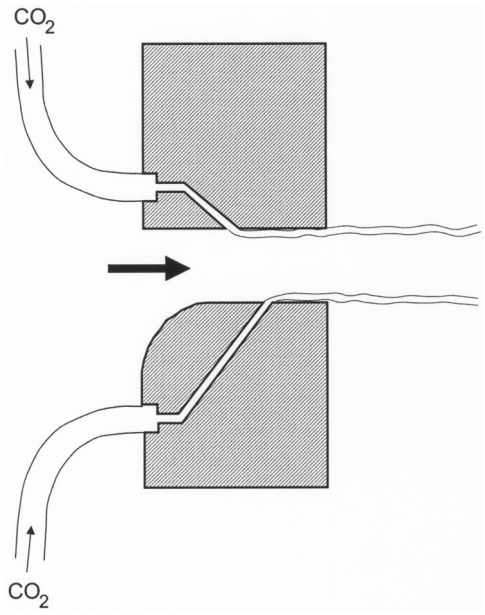


FIG. 14. Scheme of the slit in the blocks of the lips, used for the injection of $CO_2$ during the flow visualization.

tion amplitudes. This behavior does not occur for the other mouth geometries considered or is much less pronounced.

From Fig. 10, the two types of behavior of the flow in the mouth of the resonator, which were described in Sec. II, are pointed out. For high ratios $W/h$ $(W/h>2)$, the jet formed at the exit of the flue channel is thin and the flow behavior can be described by the jet-drive model presented in Sec. II. For smaller ratios $W/h$ $(W/h<2)$, the jet becomes too thick to remain in one bulk and it breaks down in two ''independent'' shear layers. This is described by the discrete-vortex model (Sec. II).

For thin jets $(W/h>2)$, the relation deduced by Verge *et al.* (1997a, b) from the jet-drive model (Verge *et al.* 1994a) is checked [Eq. (13)] in Fig. 11. The points represent the experimental data and the lines correspond to a least-square fit of the experimental data. We see that the proportionality between $(|d\xi/dt|_{\max}/U_0)^2$ and $S_r(h/W)^{3/2}$ is indeed a fair approximation of the behavior for thin jets. For the 15°-labium in the case of a flue exit with sharp edges (▽), we observe more scatters around this ideal than for the other mouth geometries. As discussed above, the sound production was rather unstable in that particular case.

### 2. Comparison with the simple model proposed

Figure 12 shows the prediction of the maximum of the pulsation amplitudes $(|d\xi/dt|/U_0)_{\max}$ as a function of the ratio $W/h$ for a flue exit with chamfered edges and the 15°-labium. The analytical data obtained from the simple model described in Sec. II are compared to experimental results.

The model is able to predict the two expected types of behavior as a function of the jet thickness $h$ compared to the mouth width $W$. This model could be improved by taking into account the flow separation induced at the labium by the passage of vortices (Fig. 13).

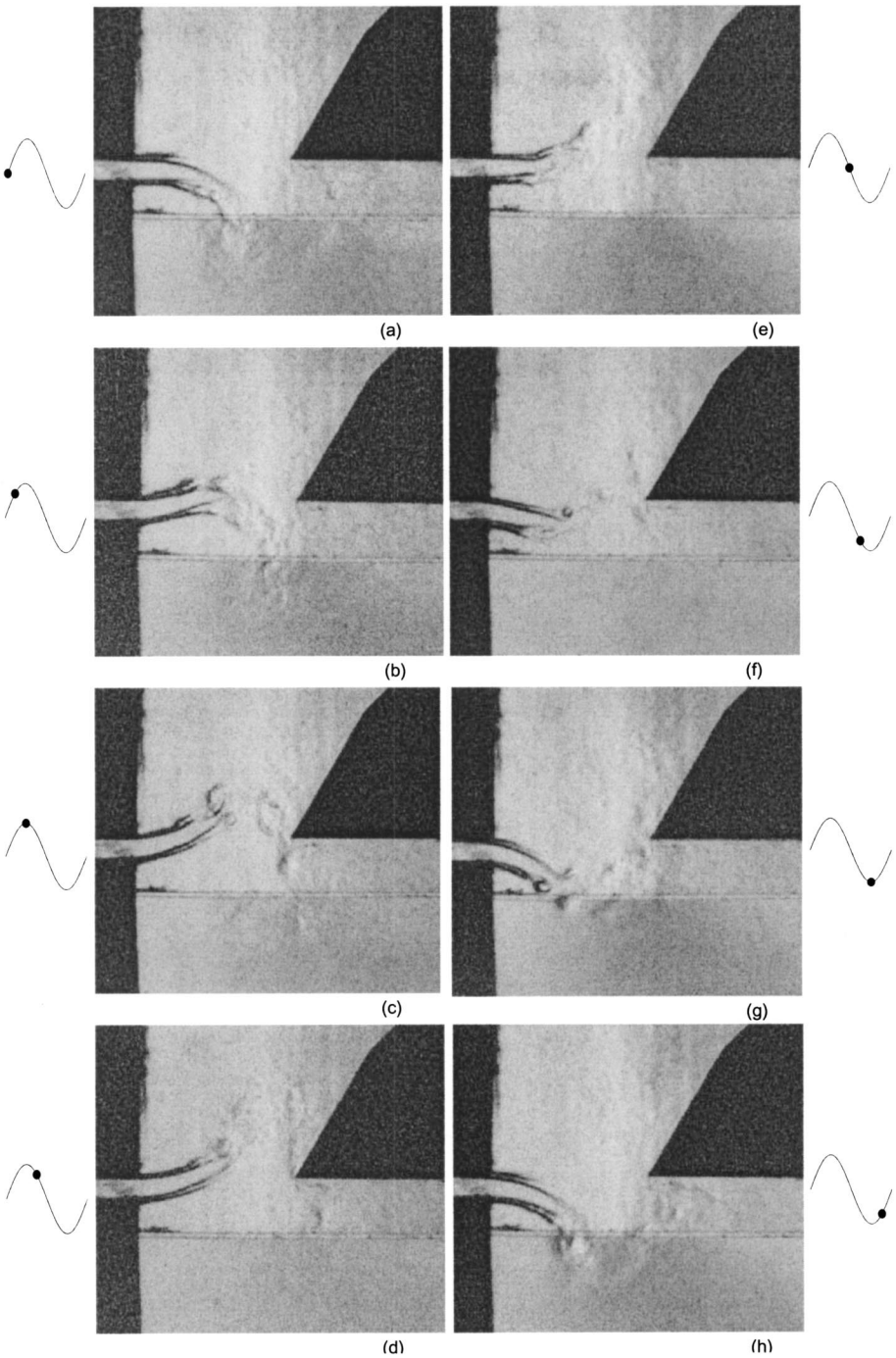


FIG. 15. Vortex shedding in the mouth of the resonator with the 60°-labium, a flue exit with sharp edges, and a channel height $h=4$ mm ($W/h=6$) ($L=552$ mm, $U_0=16.26$ m/s, $S_r=0.19$). The jet swings around the labium and enters entirely into the resonator during part of the oscillation cycle. The time, at which each picture is taken, is shown on the acoustical velocity signal. The pictures (a)–(h) are at $t/T=0.002,0.13,0.25,0.37,0.50,0.63,0.75,0.88$, respectively. The origin $t/T=0$ is the point at which the sign of the acoustical velocity becomes positive.

### C. Flow visualization

The periodic flow in the mouth of the resonator is visualized by means of a standard schlieren technique (Merzkirch, 1987).

A lens is placed at each side of the mouth of the resonator. The source of light used is a nanolite light and is placed at the focus length of the first lens so that the beam of light is parallel between the two lenses. The nanolite spark discharge provides a light pulse of about 80 ns duration each time the acoustic pressure at the top of the resonator exceeds a certain value. An additional delay between the triggered signal and the nanolite pulse is introduced in order to visualize the flow at a different moment of the oscillation period $T$. The injection of a gas with a different refractive index in the mouth of the resonator results in the deviation of the light beam and enables the visualization of the shear layer. At the focus length of the second lens, a small diaphragm is placed in order to be able to adjust the luminosity and the contrast of the pictures. The resulting pictures are taken by means of a camera placed just behind the diaphragm.

Flow visualization has been carried out on a flue exit with sharp edges for the 60°-labium. The gas injected is $CO_2$. The injection is done by means of a slit in the blocks of the lips (Fig. 14). This slit is made at an angle of 45° in order to reduce disturbances of the shear layers.

The results are shown in Figs. 15–17 for three different

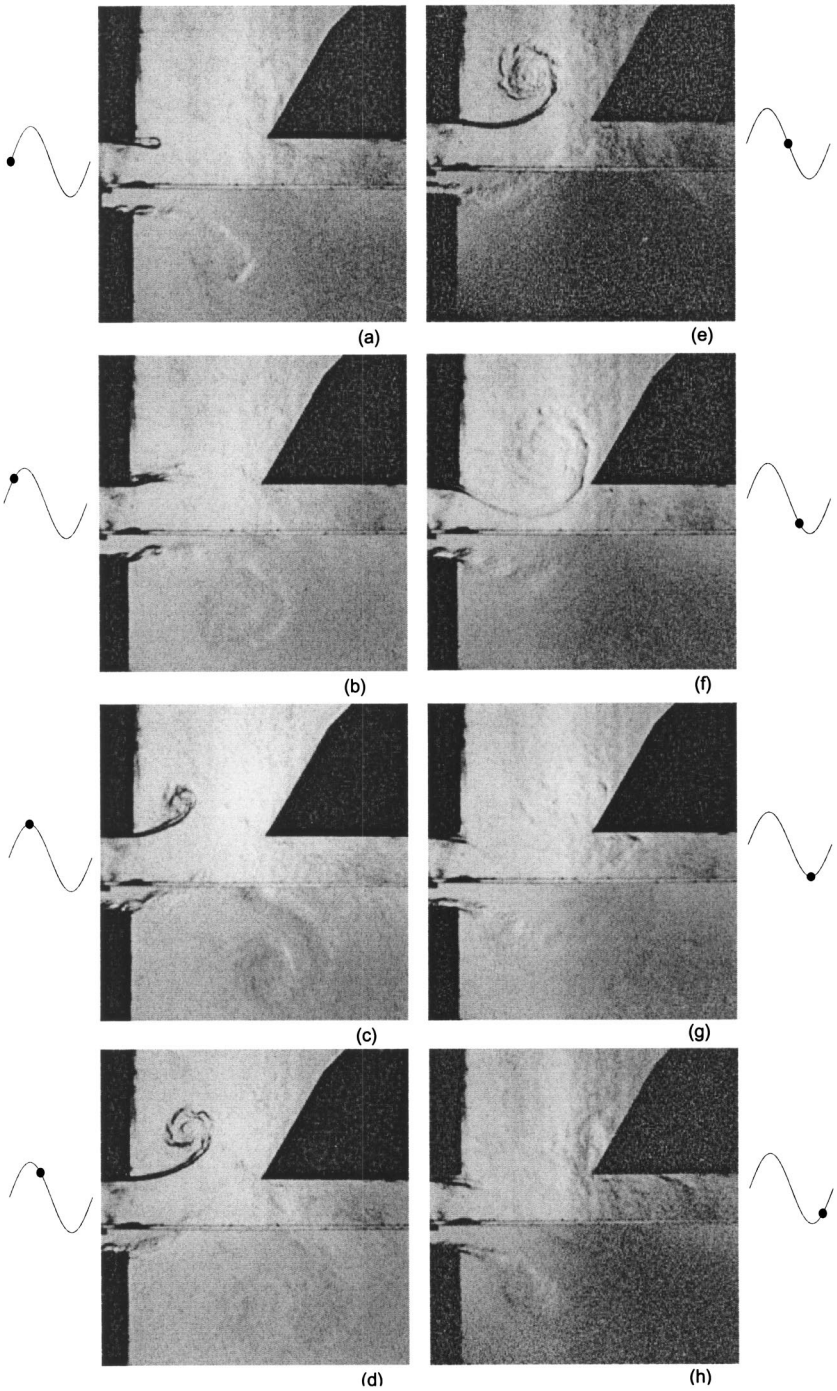


FIG. 16. Vortex shedding in the mouth of the resonator with the 60°-labium, a flue exit with sharp edges, and a channel height $h=14$ mm ($W/h=1.7$) ($L=552$ mm, $U_0=14$ m/s, $S_r=0.22$). We are near the transition $W/h=2$ between the jet-drive behavior and the individual shear layer behavior. The time, at which each picture is taken, is shown on the acoustical velocity signal. The pictures (a)–(h) are at $t/T=0,0.12,0.25,0.37,0.50,0.62,0.76,0.87$, respectively. The origin $t/T=0$ is the point at which the sign of the acoustical velocity becomes positive.

heights $h$ of the channel. For $W/h=6$ (Fig. 15), the jet is thin and oscillates around the labium. When the acoustical pressure at the top of the resonator is minimal, the acoustical velocity starts entering the resonator and the jet is directed into the resonator during half an oscillation period. During the second half of the oscillation period, the acoustical velocity changes sign and the jet is directed out of the resonator.

For $W/h=1.7$ (Fig. 16) and $W/h=0.8$ (Fig. 17), the jet breaks down into two independent shear layers. The lower shear layer does not enter into the resonator. The jet-drive model certainly fails in these cases. When the acoustical velocity is positive (enters the resonator), a first vortex is formed at the upper side of the lips. Half an oscillation period later, a second vortex is formed at the lower side of the lips. Only the first hydrodynamic mode was visualized. For higher Strouhal numbers (smaller main flow velocity), higher hydrodynamic modes can be visualized (Fig. 18).

## IV. CONCLUDING REMARKS

The recorder has a relatively poor acoustical response for higher harmonics compared to the transverse flute. We expect that the very sharp labium (15°-labium) of the recorder will generate strong higher harmonics in the source spectrum due to impulsive vortex shedding at the tip of the labium (Verge *et al.*, 1994b; Nolle, 1983). A turbulent jet would in such a case produce a very noisy sound which is

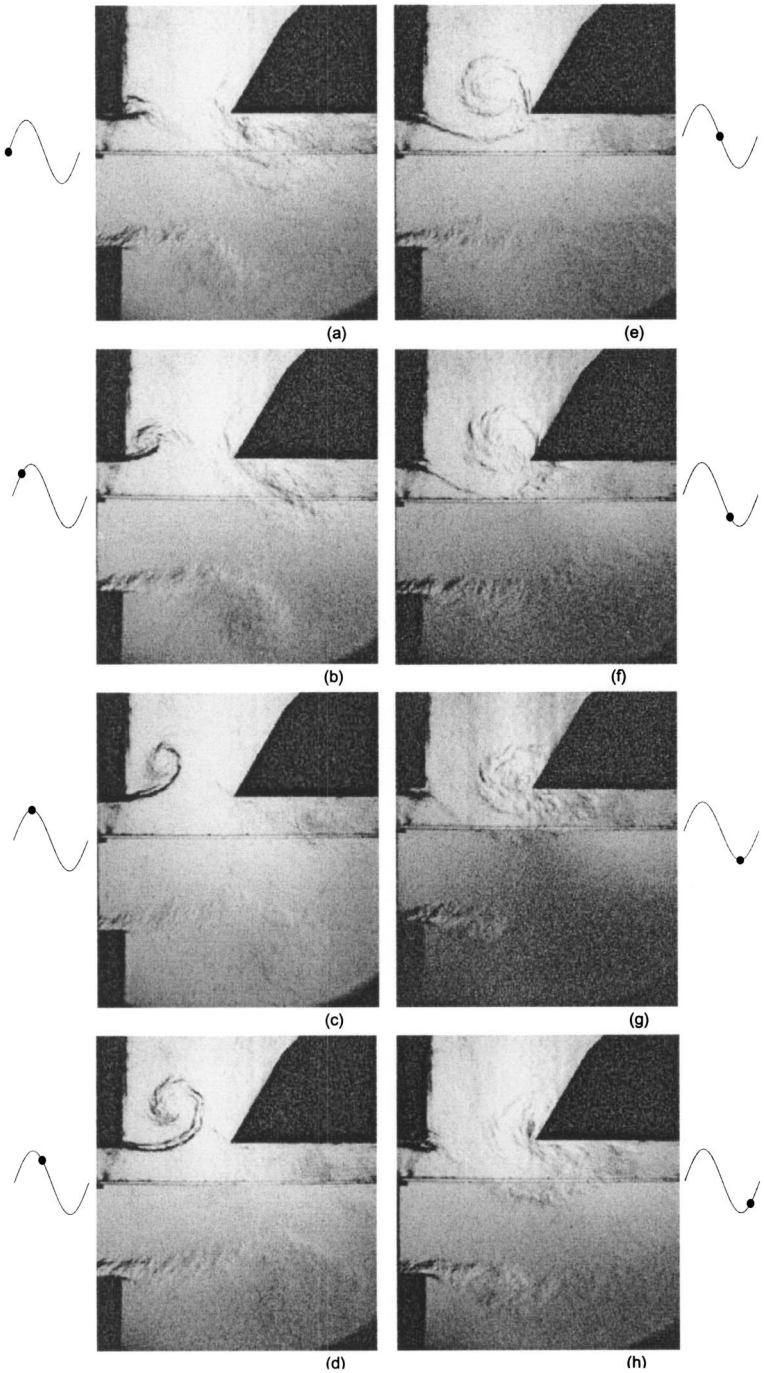


FIG. 17. Vortex shedding in the mouth of the resonator with the 60°-labium, a flue exit with sharp edges, and a channel height $h=30$ mm ($W/h=0.8$) ($L=552$ mm, $U_0=14.5$ m/s, $S_r=0.22$). The outer shear layer remains far away from the opening of the resonator. The time, at which each picture is taken, is shown on the acoustical velocity signal. The pictures (a)–(h) are at $t/T=0,0.12,0.25,0.35,0.45,0.6,0.75,0.85$, respectively. The origin $t/T=0$ is the point at which the sign of the acoustical velocity becomes positive.

avoided by keeping the blowing pressure of the instrument low. This is at the expense of the power of the instrument. In a transverse flute (Boehm flute), the excellent harmonicity of higher modes results in a rich sound even for a thick labium with an angle of 60°. This has the advantage of a reduction of turbulent noise at a given blowing pressure but also appears to provide a more stable jet oscillation for thick jets. As the flute operates with a variable jet thickness (lips of the musician), this could be an additional argument to use a labium with a large angle (60°).

Two simplified source models for flue instruments have been proposed. The models explain the variation of the oscillation amplitudes as a function of the ratio $W/h$ of the mouth width $W$ to the jet thickness $h$ for low Strouhal numbers. The jet-drive model (Coltman, 1976) is valid for thin jets ($W/h>2$) which are typically present in musical instruments. A discrete-vortex model, inspired by the works of Holger *et al.* (1977) and Meissner (2002), has been proposed to explain the sound production of the instrument when the jet-drive model fails ($W/h<2$). These two models can be combined in a global model which could be used in a sound synthesis model if the jet-drive model is complemented with a model predicting the effect of the sound source relative to the acoustical oscillation. In first approximation, a simple delay line could be considered. Alternatively, the approach of Fletcher and Rossing (1998) could be used. It is furthermore clear that our model will not predict accurately the spectral envelope of the sound produced by the instrument. Finally,

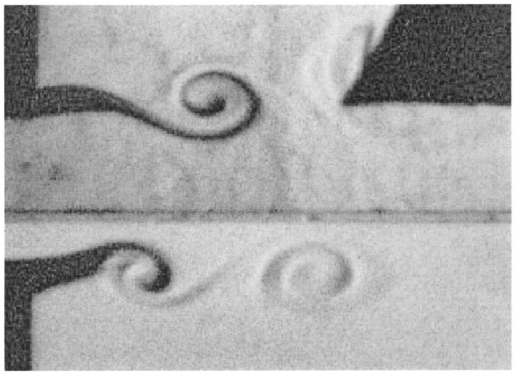

FIG. 18. Visualization of the second hydrodynamic mode in the mouth of the resonator with the 60°-labium, a flue exit with sharp edges, and a channel height $h=14$ mm ($W/h=1.7$) (length of the resonator: $L=552$ mm).

we would like to mention that we are now studying the effect of the acoustics of the instrument on the sound source. Preliminary results show no major effects of the acoustics on the flow.


Brown, C. E., and Michael, W. H. (**1954**). ''Effect of Loading Edge Separation on the Lift of a Delta Wing,'' J. Aeronaut. Sci. **21**, 690–695.

Bruggeman, J. C., Hirschberg, A., van Dongen, M. E. H., Wijnands, A. P. J., and Gorter, J. (**1989**). ''Flow Induced Pulsations in Gas Transport Systems: Analysis of the Influence of Closed Side Branches,'' J. Fluids Eng. **111**, 484–491.

Campbell, M., and Greated G. (**1987**). *The Musician's Guide to Acoustics* (Schirmer, New York).

Castellengo, M. (**1976**). ''Contribution à l'étude expérimentale des tuyaux à bouche,'' Ph.D. thesis, Université de Paris VI, Paris.

Coltman, J. W. (**1966**). ''Resonance and sounding frequencies of the flute,'' J. Acoust. Soc. Am. **40**, 99–107.

Coltman, J. W. (**1968**). ''Sounding mechanism of the flute and organ pipe,'' J. Acoust. Soc. Am. **44**, 983–992.

Coltman, J. W. (**1969**). ''Sound radiation from the mouth of an organ pipe,'' J. Acoust. Soc. Am. **46**, 477.

Coltman, J. W. (**1976**). ''Jet drive mechanism in edge tones and organ pipes,'' J. Acoust. Soc. Am. **60**, 725–733.

Coltman, J. W. (**1980**).

Crighton, D. G. (**1992**). ''The Edge Tone Feedback Cycle. Linear Theory for the Operating Stages,'' J. Fluid Mech. **234**, 361–391.

Dequand, S. (**2001**). ''Duct Aeroacoustics: from Technological Applications to the Flute,'' Ph.D. thesis, Technische Universiteit Eindhoven, Netherlands and Université du Maine, France.

Dequand, S., Luo, X., Willems, J. F. H., and Hirschberg, A. (**2001**). ''Self-Sustained Oscillations in a Helmholtz-like Resonator. Part 1: Acoustical Measurements and Analytical Models,'' in *7th AIAA/CEAS Aeroacoustics Conference* (Maastricht, Nl), submitted to the AIAA Journal.

Elder, S. A. (**1973**). ''On the mechanism of sound production in organ pipes,'' J. Acoust. Soc. Am. **54**, 1554–1564.

Elder, S. A. (**1992**). ''The Mechanism of Sound Production in Organ Pipes and Cavity Resonators,'' J. Acoust. Soc. Jpn. (E) **13**, 11–23.

Fabre, B., and Hirschberg, A. (**2000**). ''Physical Modelling of Flue Instruments: a Review of Lumped Models,'' Acust. Acta Acust. **86**, 599–610.

Fabre, B., Hirschberg, A., and Wijnands, A. P. J. (**1996**). ''Vortex Shedding in Steady Oscillations of a flue Organ Pipe,'' Acust. Acta Acust. **82**, 863–877.

Fletcher, N. (**1976**). ''Jet drive mechanism in organ pipes,'' J. Acoust. Soc. Am. **60**, 481–483.

Fletcher, N. (**2002**). Private communication.

Fletcher, N., and Rossing, T. (**1998**). *The Physics of Musical Instruments* (Springer-Verlag, New York).

Hirschberg, A. (**1995**). ''Aeroacoustics of Wind Instruments'' in *Mechanics of Musical Instruments*, International Centre for Mechanical Sciences, Courses and Lectures No. 35, edited by Hirschberg A., Kergomard J., and Weinrich (Springer-Verlag, Wien), pp. 291–369.

Holger, D. K., Wilson, T. A., and Beavers, G. S. (**1977**). ''Fluid mechanics of the edge-tone,'' J. Acoust. Soc. Am. **62**, 1116–1128.

Howe, M. S. (**1975**). ''Contributions to the Theory of Aerodynamic Sound, with Application to Excess Jet Noise and the Theory of the Flute,'' J. Fluid Mech. **71**(4), 625–673.

Howe, M. S. (**1980**). ''The Dissipation of Sound at an Edge,'' J. Sound Vib. **70**, 407–411.

Howe, M. S. (**1998**). *Acoustics of Fluid-Structure Interactions* (Cambridge U.P., Cambridge).

Ingard, K. U., and Ising, H. (**1967**). ''Acoustic nonlinearity of an orifice,'' J. Acoust. Soc. Am. **42**, 6–17.

Mattingly, G., and Criminale, W. (**1971**). ''Disturbance characteristics in a plane jet,'' Phys. Fluids **14**, 2258–2264.

Meissner, M. (**2002**). ''Aerodynamically Excited Acoustic Oscillations in Cavity Resonator Exposed to an Air Jet,'' Acust. Acta Acust. **88**, 170–180.

Merzkirch, W. (**1987**). *Flow Visualization*, 2nd ed. (Academic, London).

Nederveen, C. J. (**1998**). *Acoustical Aspects of Woodwind Instruments*, 2nd ed. (Northern Illinois U.P., De Kalb).

Nelson, P. A., Halliwell, N. A., and Doak, P. E. (**1983**). ''Fluid Dynamics of a Flow Excited Resonance. Part 2: Flow Acoustic Interaction,'' J. Sound Vib. **91**, 375–402.

Nolle, A. W. (**1983**). ''Flue organ pipes: Adjustments affecting steady waveform,'' J. Acoust. Soc. Am. **73**, 1821–1832.

Peters, M. C. A. M. (**1993**). ''Aeroacoustic Sources in Internal Flows,'' Ph.D. thesis, Technische Universiteit Eindhoven.

Powell, A. (**1961**). ''On the edge-tone,'' J. Acoust. Soc. Am. **33**, 395–409.

Pullin, D. I. (**1978**). ''The large scale structure of unsteady self-similar rolled-up vortex sheets,'' J. Fluid Mech. **88**, 401–430.

Ségoufin, C., Fabre, B., Verge, M. P., Hirschberg, A., and Wijnands, A. P. J. (**2000**). ''Experimental Study of the Influence of the Mouth Geometry on Sound Production in a Recorder-like Instrument: Windway Length and Chamfers,'' Acust. Acta Acust. **86**, 649–661.

Ségoufin, C., Fabre, B., and Thiria, B. (**2001**). ''Experimental Confrontation of Linear and Non-Linear Jet Theories Production in Recorder Type Instrument,'' in *Proceedings of the International Symposium on Musical Acoustics ISMA*, Vol. 1, Perugia, Italy.

Verge, M. P., Caussé, R., Fabre, B., Hirschberg, A., Wijnands, A. P. J., and van Steenbergen, A. (**1994**). ''Jet Oscillations and Jet Drive in Recorder-like Instruments,'' Acta Acust. united with Acustica **2**, 403–419.

Verge, M. P., Fabre, B., and Hirschberg, A. (**1994b**). ''Jet formation and jet velocity fluctuations in a flue organ pipe,'' J. Acoust. Soc. Am. **95**, 1119–1132.

Verge, M. P., Fabre, B., Hirschberg, A., and Wijnands, A. P. J. (**1997a**). ''Sound production in a recorder-like instrument. Part 1: Dimensionless amplitude of the internal acoustic field,'' J. Acoust. Soc. Am. **101**, 2914–2924.

Verge, M. P., Fabre, B., Hirschberg, A., and Wijnands, A. P. J. (**1997b**). ''Sound production in a recorder-like instrument. Part 2: A simulation model,'' J. Acoust. Soc. Am. **101**, 2925–2939.

Wolfe, J., Smith, J., and Fletcher, N. H. (**2001**). ''Acoustic Impedance Spectra of Classical and Modern Flutes,'' J. Sound Vib. **243**, 127–144.